ExBoX: a simple Boolean exclusion strategy to drive expression in neurons

Running title: Neuronal expression by Boolean Exclusion

Tyler Vahedi-Hunter*[1], Teresa Ubina*[1], Akshay Gupta[1], Wenny Wong[1], Will Agnew-Svoboda[1], Vijayalakshmi Santhakumar[1], Martin M. Riccomagno[1]

[1] Neuroscience Graduate Program, Department of Molecular, Cell & Systems Biology, University of California, Riverside, CA, USA

*Authors contributed equally to this work

Corresponding Author: Martin M. Riccomagno, martinmr@ucr.edu.

Keywords: Boolean logic, recombinases, combinatorial expression, intersectional approaches, Cre, Flp, Adeno-Associated Virus.

Abstract

The advent of modern single-cell biology has greatly enhanced our understanding of the striking diversity within cell populations that previously appeared homogenous. This newly appreciated complexity has made intersectional genetic approaches essential to understanding and probing cellular heterogeneity at the functional level. Here we build on previous knowledge to develop a simple AAV-based approach to define specific subpopulations of cells by Boolean exclusion logic (AND NOT). This Expression by Boolean Exclusion (ExBoX) system encodes for a gene of interest which is turned on by a particular recombinase (Cre or FlpO) and turned off by another. ExBoX allows for the specific transcription of a gene of interest in cells expressing only the activating recombinase, but not in cells expressing both. We show the ability of the ExBoX system to tightly regulate expression of fluorescent reporters both in vitro and in vivo, and further demonstrate the powerful adaptability of the system by achieving expression of variety of virally-delivered coding sequences in the mouse brain. This simple strategy will expand the molecular toolkit available for cell- and time-specific gene expression in a variety of organisms and systems.

Abbreviations:

Hemagglutinin (HA)

Adeno-Associated Virus (AAV)

Double-floxed Inverse Orientation (DIO)

Dentate Gyrus (DG)

Gene Of Interest (GOI)

Introduction

Advancements in our understanding of the mechanisms underlying biological processes have been greatly dependent on the development of new genetic tools. A big breakthrough in mammalian genetics was the discovery and implementation of homologous recombination to generate loss-of-function alleles in mice (Capecchi, 1989). The introduction of recombinases as genetically encoded tools, in combination with conditionally targeted genetic alleles, made the control of genetic deletion in a tissue-specific manner possible (Gu et al, 1994; Tsien et al, 1996). With the availability of recombinase-dependent systems, region-specific gene knockouts and progenitor tracing have now become routine experimental strategies in mouse genetics (Branda & Dymecky, 2004).

Although cell diversity has always been appreciated in biology, single-cell profiling has revolutionized the way we think about certain organs by uncovering cell heterogeneity in populations that were once thought to display less complexity (Darmanis et al, 2015). Our ability to appreciate cellular complexity is currently limited by the available tools to label and manipulate cells with increased specificity. One way to overcome this limitation is to simply expand the pool of tissue- and population-specific recombinase lines. This requires the generation and characterization of independent transgenic recombinase mouse lines for each newly discovered cell population. A complementary approach that can take advantage of preexisting transgenic lines is to incorporate genetically encoded intersectional approaches (Awatramani et al, 2003). In comparison to conventional transgenic strategies that select cellular targets based on expression of one particular promoter or driver,

intersectional approaches provide tighter specificity by selecting targets based on the overlapping or sequential expression of multiple recombinases (Jensen & Dymecki, 2014). These intersectional strategies based on the combinatorial expression of two recombinase systems (Cre/lox and Flp/FRT) were first used in the mouse to perform fate mapping of previously elusive neural progenitors (Dymecki, Ray, & Kim 2010). Intersectional approaches are not only able to label subpopulations with greater specificity, but also make a variety of Boolean logic operations (AND, NOT, OR) available (Daigle et al., 2019; Plummer et al, 2015). With multiple recombinase systems driving the expression of reporter genes, targeting of subpopulations of cells can be achieved through intersectional (expressing all drivers) and subtractive (lacking expression of one or more drivers) strategies (Farago et al, 2006).

Viral vectors offer an alternative approach to driving conditional and intersectional expression (Schnütgen et al, 2003; Atasoy et al, 2008; Gradinaru 2010; Fenno et al, 2014). Strictly genetically encoded strategies have clear advantages over surgically introduced viral vectors, like non-invasiveness and broad applicability in hard to reach tissues during otherwise inaccessible embryonic stages (Jensen & Dymecki, 2014). However, viral expression systems can be extremely powerful given the ease of generation, and the additional level of control one can gain by selecting the region and time of injection (Zhang et al, 2007; Sternson et al, 2015). There are now multiple versions of recombinase-dependent AAVs for recombinases like Cre, Flp, and DRE (Atasoy et al, 2008; Saunders et al, 2012; Xue, Atallah, & Scanziani, 2014). More recently, systems for intersectional expression driven by AAVs have also been developed (Kakava-Georgiadou et al, 2019; Fenno et al, 2014). Combination of these

viral and genetically-encoded approaches will ultimately be essential to understand whether newly discovered molecular diversity within cell populations amounts to any notable phenotypic difference in terms of cellular structure and function.

In addition to being able to parse out functional diversity, there is an interest in the field of developmental biology in being able to specifically turn genes on and off during defined developmental windows or critical periods (Wiesel & Hubel,1963, Kozorovitskiy et al, 2012). Intersectional approaches using Boolean negation/exclusion could provide a solution to this problem: a gene of interest could be turned on by a particular recombinase at a particular time point, while turned off later (AND NOT) by a different recombinase (Table 1). Although a sophisticated system for AAV-driven expression using exclusion logic has been generated elsewhere (Fenno et al, 2014), the existing vectors have limitations in terms of being unnecessarily long and intricate in design, somewhat restricting their applicability. In this study we describe the design and characterization of an alternative expression system governed by Boolean exclusion logic and driven by a single AAV. The newly developed vectors are simpler in design and smaller in size, allowing for expression of longer genes of interest (GOI). As proof of principle, we validated the system in neuronal populations, and also generated tools for regulating neuronal activity in vivo.

Results

Design and construction of a combinatorial expression system using Boolean exclusion: CreOn-FlpOff ExBox

To control expression and label subsets of cells with greater specificity using Cre and FLP recombinases, we set out to develop a simple AAV-based expression system governed by Boolean Exclusion logic (Expression by Boolean Exclusion or ExBoX). We first generated a system in which expression of a coding sequence of interest is turned ON by Cre recombinase and turned OFF by Flp recombinase: CreOn-FlpOff (Table 1). The CreOn-FlpOff vector was designed to contain a cassette with a coding sequence (CDS) of interest in-frame with a hemagglutinin tag (HA), P2A site, and EGFP reporter inverted with respect to a promoter. The promoter chosen for these experiments was that of human Synapsin I, which is a well characterized postmitotic neuronal promoter (Glover et al., 2002). The inverted cassette is flanked by Frt sites, and double-lox sites (lox2722 and loxP) in inverse orientation (DIO) (Schnütgen et al., 2003) (Figure 1A). Upon Cre-mediated recombination, and HA-tagged coding sequence of interest and EGFP get locked into the forward orientation, allowing for robust Cre-dependent expression in neurons. Conversely, in the presence of Flp, the cassette is excised, resulting in abolishment of CDS and EGFP reporter expression (Figure 1A). Thus, the CDS is expressed only in the presence of Cre AND NOT FlpO (Table 1).

For proof of concept, we first generated a plasmid carrying only EGFP in the reversible cassette of the CreOn-FlpOff system. The CreOn-FlpOff-EGFP plasmid was co-transfected with Cre recombinase, FlpO recombinase, or both Cre and FlpO in a neuroblastoma-derived cell line, Neuro2A (Figure 1B, left). A plasmid driving mCherry

under a constitutive promoter was co-transfected as transfection control. Upon transfection of the CreOn-FlpOff-EGFP plasmid alone, no EGFP expression is found in any cells. As expected, when CreOn-FlpOff-EGFP plasmid is co-transfected with Cre, the EGFP cassette is inverted to the correct orientation and 93.9%±0.3 of transfected cells express EGFP (Figure 1B). When CreOn-FlpOff-EGFP plasmid was co-transfected with Flp, or co-transfected with Cre and Flp, no cells expressed EGFP, suggesting that Flp can efficiently turn off reporter expression (Figure 1B). This confirms that expression from CreOn-FlpOff ExBoX vectors can be successfully manipulated through Boolean exclusion in N2A cells.

Design of a complementary system that is turned on by Flp and turned off by Cre: FlpOn-CreOff ExBox

We next generated a complementary system that is turned on by Flp and off by Cre, FlpOn-CreOff (Table 1). FlpOn-CreOff was designed using a similar internal logic, where an expression cassette containing a CDS, an in-frame HA tag, P2A site, and TdTomato reporter, are inverted with respect to the promoter. This expression cassette is flanked by lox2722 sites, and a Flp controlled DIO switch (fDIO or fFLEX) (Xue et al, 2014) containing F14 and Frt sites (Figure 2A). In this system, Flp inverts the cassette, resulting in CDS and TdTomato reporter expression, while Cre excises the cassette, causing the abolishment of CDS and TdTomato reporter expression (Figure 2A). Thus CDS expression should only occur when FlpO is present AND NOT Cre (Table 1).

As an initial proof-of-principle design, a FlpOn-CreOff vector driving simply a TdTomato fluorescent reporter was generated. FlpOn-CreOff-TdTomato plasmid was co-transfected with Cre, FlpO, or both Cre and FlpO. EGFP expressing plasmid was

used as transfection control. When the FlpOn-CreOff-TdTomato plasmid was co-transfected with FlpO, approximately 85.8%±5.6 of transfected cells displayed TdTomato expression (Figure 2B). When FlpOn-CreOff-TdTomato plasmid was co-transfected with Cre alone, there were no TdTomato expressing cells. Finally, as expected, co-transfection of the FlpOn-CreOff-TdTomato plasmid with both Cre and FlpO resulted in no TdTomato reporter expression, confirming that Cre recombinase can abolish expression of this constructs even in the presence of Flp (Figure 2B). Therefore, expression of the construct occurs only in the presence of Flp AND NOT Cre (Table 1).

Characterization of the ExBoX system in neurons

To test whether this newly developed system was able to drive expression in neurons, we tested these constructs in primary cortical cultures. We used the same plasmid combinations that were used in Neuro2A cells to perform ex-utero electroporation prior to plating. Primary neuronal cultures were observed at 3 days in vitro (DIV). Transfection of CreOn-FlpOff-EGFP plasmid alone resulted in no reporter expression (Figure 3A). Notably, co-transfection of CreOn-FlpOff-EGFP plasmid with Cre resulted in 100%±0.0 of transfected neurons expressing EGFP as expected (Figure 3A). When CreOn-FlpOff-EGFP plasmid was co-transfected with FlpO or with FlpO and Cre, we found no EGFP reporter expression in any transfected cells (Figure 3A). Similarly, transfection of FlpOn-CreOff-TdTomato plasmid alone resulted in no reporter expression (Figure 3B). Co-transfection of FlpOn-CreOff-TdTomato plasmid with FlpO resulted in 92.1%±2.0 of transfected cells expressing the TdTomato reporter, as expected (Figure 3B). If FlpOn-CreOff-TdTomato plasmid is co-transfected with Cre

alone, or Cre and FlpO, it is expected that there will be no TdTomato expression since Cre should excise the cassette. As predicted, no cells transfected in this combination had any TdTomato expression (Figure 3B).

We then tested the neuronal expression of the ExBoX system *in vivo.* Initial validation of CreOn-FlpOff was performed by *in utero* electroporation of CreOn-FlpOff-EGFP plasmid with Cre, with FlpO, or with Cre and FlpO into the lateral ventricle in E15.5 mice, followed by visualization 48 hours later. mCherry-expressing plasmids were used as electroporation controls. When the CreOn-FlpOff-EGFP plasmid was electroporated alone or with FlpO, we found no EGFP expression (Figure 4A). Tissue co-transfected with CreOn-FlpOff-EGFP plasmid and Cre had robust expression of the EGFP reporter, resulting in labeling of 97.7%±0.9 of transfected cells (Figure 4A). Co-electroporation of CreOn-FlpOff-EGFP plasmid with Cre and FlpO resulted in negligible EGFP expression (1.7%±0.9 of transfected cells, Figure 4A).

To validate FlpOn-CreOff, we electroporated the FlpOn-CreOff-TdTomato plasmid alone and this resulted in no TdTomato expression. A plasmid driving EGFP under the pCAG promoter was used as electroporation control. Co-electroporation of FlpOn-CreOff-TdTomato plasmid with FlpO resulted in inversion of the cassette and detectable expression of TdTomato in 86.9%±3.1 of transfected cells (Figure 4B). Co-electroporation of FlpOn-CreOff-TdTomato plasmid with Cre showed no TdTomato expression (Figure 4B). Finally, no TdTomato expression was detected when the FlpOn-CreOff-TdTomato plasmid was co-electroporated with FlpO and Cre, indicating successful AND NOT exclusion (Figure 4B). These data suggest that FlpOn-CreOff and CreOn-FlpOff ExBoX work efficiently in neurons, *in vitro* and *in vivo*.

Validation of ExBoX AAVs *in vivo*

To generate tools that would be useful for manipulation of gene expression in the postnatal brain, we packaged the FlpOn-CreOff construct into AAV9. To validate that expression of the FlpOn-CreOff constructs is maintained in the virally-packaged form, we performed stereotactic injections to deliver FlpOn-CreOff-TdTomato AAV into the dentate gyrus (DG) of adult mice *in vivo*. FlpOn-CreOff-TdTomato AAV was co-injected with either AAV-EF1α-FlpO-WPRE (AAV-EF1α-FlpO), or with AAV-EF1α-FlpO and pENN.AAV.CamKII 0.4. Cre. SV40 (AAV-CamkII-Cre), and expression was observed after 3 weeks (Figure 5). AAV expressing EGFP was co injected in WT and when Cre was injected to visualize the injection site. Similar to our previous findings with FlpOn-CreOff plasmids, robust TdTomato reporter expression was observed in DG neurons co-infected with AAV-FlpOn-CreOff-TdTomato and AAV-EF1α-FlpO (Figure 5A, C), verifying that expression of the construct in the presence of the ‘ON’ recombinase was maintained in viral form. Furthermore, AAV-FlpOn-CreOff-TdTomato reporter expression was inactivated by CamkII-Cre even in the presence of AAV-EF1α-FlpO (Figure 5B, D; Figure S1). Thus, the FlpOn-CreOff construct works as expected when packaged into AAV9.

We next packaged the complementary CreOn-FlpOff construct into AAV9. To validate that expression of the CreOn-FlpOff construct is maintained in the virally-packaged form, we performed stereotactic injections to deliver CreOn-FlpOff-EGFP AAV into the dentate gyrus (DG) of adult mice *in vivo*. For validation for the viral CreOn-FlpOff construct we incorporated a genetically-encoded Cre recombinase driven by a

transgene. The *Grik4-cre* mouse line was specifically chosen for providing robust Cre expression in the hippocampus, including the DG (Supplemental Figure S2). AAV-CreOn-FlpOff-EGFP was injected independently *Grik4-Cre* mice or Cre-negative littermates (WT), or co-injected with AAV-EF1α-FlpO into *Grik4-Cre* animals (Figure 6). AAV9 constitutively expressing TdTomato (pAAV-CAG-TdTomato) was co-injected in WT animals and with the AAV-EF1α-FlpO injection to visualize the injection site. When AAV-CreOn-FlpOff-EGFP was injected into WT (Cre-negative) animals, no EGFP reporter expression was observed (Figure 6A, D, G). Conversely, injections into *Grik4-Cre* positive animals demonstrated robust EGFP reporter expression (Figure 6B, E, H), verifying the Cre-dependent activation of the virally-packaged construct. Furthermore, in *Grik4-Cre* animals co-injection of AAV-EF1α-FlpO resulted in inactivation of EGFP reporter expression (Figure 6C, F; Supplemental Figure S1). These results suggest that the virally-packaged ExBoX constructs are successful at driving gene expression through the expected AND NOT Boolean operation.

Generation of Activity-modulating CreOn-FlpOff Viruses for Neuroscience

To further validate the ExBoX system using multiple different cargos, we next generated CreOn-FlpOff AAV constructs co-expressing EGFP and well-characterized modulators of neuronal firing or synaptic release. To reduce activity, we generated a CreOn-FlpOff virus that expresses Kir2.1 (AAV-CreOn-FlpOff-Kir2.1-EGFP), an inward-rectifying K+ channel that has been demonstrated to increase rheobase current and reduce resting membrane potential of neurons when overexpressed (Xue et al, 2014). In parallel, we cloned a version of Kir2.1 carrying three point mutations that render the

channel in a non-functional state, referred to as Kir2.1Mut (AAV-CreOn-FlpOff-Kir2.1Mut-EGFP) (Xue et al, 2014), which can be used as negative control for the Kir2.1 construct. We also designed a CreOn-FlpOff virus encoding mNaChBac (AAV-CreOn-FlpOff-mNaChBac-EGFP). This bacterial Na^+ ion channel has been demonstrated to increase firing of neurons when overexpressed by reducing action potential threshold and rheobase (Xue et al, 2014). To serve as negative control for mNaChBac in neural circuit experiments, we cloned a non-conducting mNaChBac mutant referred to as mNaChBacMut into the CreOn-FlpOff vector (AAV-CreOn-FlpOff-mNaChBacMut-EGFP) (Xue et al, 2014). Finally, we generated CreOn-FlpOff encoding tetanus toxin (AAV-CreOn-FlpOff-TeTN-EGFP) to block synaptic transmission (Sweeney et al, 1995).

We validated reporter expression of these five viral constructs in adult mice using stereotactic injection to deliver each independently or in combination with AAV-EF1α-FlpO into the DG of adult Grik4-Cre mice or WT (Cre-negative) littermates (Figure 7). To visualize the injection site pAAV-Syn-mCherry was co-injected in WT, or when AAV-EF1α-FlpO was injected. As expected, injection of any of the viral constructs into Cre-negative animals produced no EGFP reporter expression (Figure 7A, E, I, M, Q). Conversely, each virus was able to produce robust EGFP reporter expression in DG neurons when injected into Grik4-Cre positive animals (Figure 7B, F, J, N, R), demonstrating expression of these viral constructs is Cre-dependent. Furthermore, in *Grik4-Cre* mice injection of AAV-EF1α-FlpO prevented EGFP reporter expression (Figure 7C, D, G, H, K, L, O, P, S, T; Supplemental Figure S3). Thus, despite the larger cargo size, expression of these activity-modulating CreOn-FlpOff viral constructs was similar to that of the CreOn-FlpOff-EGFP viral construct (Figure 6). Overall, our data

suggest that the ExBoX system can be used to efficiently control expression of multiple genes of interest in a Cre- and Flp-dependent manner through AND NOT Boolean operations.

Discussion

Design of a simpler, more space-efficient Boolean exclusion expression system

The ability to identify and characterize specific cell types and subpopulations has been challenging in part because, until recently, cell targeting strategies have been limited to populations defined by expression of a single marker or reporter. In order to solve this issue and increase specificity of target selection, a number of intersectional strategies have been developed (Atasoy et al, 2008; Fenno et al, 2014; Gradinaru et al, 2010; Jensen & Dymecki, 2014; Plummer et al, 2015; Schnütgen et al, 2003). A previous study described the generation of an expression system using Boolean logical operations, all governed by a single AAV vector (Fenno et al., 2014). This system, called INTERSECT, incorporated a modular intron-containing system capable of driving transcription using multiple Boolean logical operations such as AND, NOT, AND NOT, XOR, and NAND (Fenno et al., 2014). While extremely elegant, the design for the AND NOT constructs was constrained by the fact that it followed the same internal logic as the AND INTRSECT constructs. As a result of this constraint the currently existing AND NOT system has a couple of shortcomings. The first limitation is that this system adds two introns that make the constructs longer by 194 base-pairs. This is not a serious concern when expressing from a plasmid, but it becomes relevant when dealing with viruses with limited packaging capacity like AAV (Dong et al., 1996). Another concern with the use of introns is that they make the design and cloning of other coding

sequences into these vectors more difficult and cumbersome. In this study, we generated an alternative system aimed at solving these constraints. Thus, by design, the ExBoX system has two clear advantages over previous systems: it provides more cargo room and has a simpler design, allowing for replacement of the CDS cassette in a simple cloning step.

The ExBoX system allows for robust expression only in the presence of the respective ON switch, which can be reliably inactivated in the presence of the OFF switch (Table 1). This is true for both plasmid (Figures 1-4) and viral constructs (Figures 5-7) as validated by a battery of *in vitro* and *in vivo* experiments in embryonic and postnatal tissues. Altogether, these experiments demonstrate that the ExBoX system is effective in delivering strong recombinase-dependent expression in a variety of settings.

A Boolean system to control expression with temporal and cell-type specificity

Boolean logic AND-NOT operations made available by ExBoX can be used to study previously inaccessible subpopulations. In situations where there is no suitable specific driver for a subpopulation of interest, the ExBoX system can be used to drive expression of a gene of interest or reporter in said subpopulation, provided there is a recombinase driver available for a broader neuronal population, and one for the cells to be excluded (Figure 8A). For example, the AND NOT logic of the ExBoX system could be utilized to label or genetically manipulate 5HTR3a^{+};VIP^{-} interneurons in the cortex (Tremblay et al., 2016). This could be done by turning on expression of a CreON-FlpOff construct with *HTR3a-Cre*, while excluding inhibitory neurons expressing *VIP-FlpO* (Figure 8A) (Che et al., 2018; He et al., 2017; Gerfen et al., 2013).

In addition to cell-specificity, these intersectional approaches can be used to achieve temporal control. This is particularly important when studying developmental events or degenerative diseases with defined critical periods. Using ExBoX one could take advantage of the expression of a recombinase to provide cell-type specificity, and a second recombinase to turn off expression at the desired time (Figure 8B). For example, expression of a gene of interest in the DG can be turned ON by injecting ExBoX AAVs at a desired developmental time point into *Grik4-Cre* mice, and later turned OFF with Flp, thus creating a window of expression.

The tissue- and temporal-specificity conferred by the ExBoX system will make developmental studies that were previously limited by the pre-existing tools possible. With this in mind, we generated ExBoX vectors encoding for neuronal activity and synaptic transmission modulators, which will allow for tight control of these functional manipulations in time and space. These activity-modulating tools, although well characterized in a variety of circuits (see Bando et al., 2016; Burrone et al., 2002; Johns et al., 1999; Lin et al., 2010; Okada and Matsuda, 2008; Priya et al., 2018; Sim and Antolin et al., 2013; Sweeney et al, 1995; Xue et al, 2014 for examples), will need to be validated in each particular setting and/or system. To facilitate studies where the timing of CDS expression is critical, we are currently generating AAV vectors driving expression of a tamoxifen-dependent FlpO (data not shown) (Goodrich et al, 2018). This AAV-FlpOERT2 could be delivered at the same time as the ExBoX AAVs and used to turn off expression by orally providing tamoxifen at a later timepoint.

Expanding the toolkit to study gene function

Due to the ExBoX's simple design, the system can be easily modified to incorporate alternative and/or additional recombinase systems. For example, inclusion of the Dre-Rox recombinase system, in addition to Cre-lox and Flp-frt, would provide even greater intersectional specificity (Plummer et al, 2015). In addition to Dre-ON and OFF intersectional AND NOT systems, this could theoretically enable AND-NOT-NOT Boolean logic operations, permitting an even greater expanse of possibilities. In addition, by using other promoters in the AAV constructs, this system can be used to drive expression in any cell-type or organ of interest. The broad applicability and exquisite specificity of the system would make the use of these vectors particularly useful for gene therapy applications.

In summary, we designed and generated a new set of viral tools to drive expression using Boolean exclusion logic, ExBoX. ExBoX AAVs allow for tight spatial and temporal control of transcription. These new tools are simple and can be easily modified to express any desired gene of interest. Our design also increases the space available for other coding sequences of interest, even if this increase in capacity is somewhat small (194 bps). As proof of concept, we generated a variety of vectors encoding for neuronal activity and synaptic transmission regulators that will be readily available to the neuroscience community. Based on its simplicity, we believe the ExBoX system will help universalize the use of combinatorial expression approaches. Combining these newly developed tools with genetically encoded Cre and FlpO lines, in addition to a growing variety of viral tools, will allow for cell-specific gene expression in a variety of systems.

Materials and Methods

Animals. The ICR mouse strain was purchased from Taconic. The Grik-4-Cre transgenic mouse strain was purchased from The Jackson Laboratory. Generation of the Grik4-cre transgenic mouse line has been described previously (Nakazawa et al., 2002). Mice were housed in a controlled environment maintained at approximately 22*C on a 12-hour light/dark cycle. Mouse chow and water were provided ad libitum. The day of vaginal plug observation was designated as embryonic day 0.5 (E0.5), and the day of birth as postnatal day 0 (P0). All animal procedures presented were performed according to the University of California Riverside's Institutional Animal Care and Use Committee (IACUC) guidelines and approved by UC Riverside IACUC.

Viral constructs. The CreOn-FlpOff and FlpOn-CreOff ExBoX viral constructs were designed using ApE (https://jorgensen.biology.utah.edu/wayned/ape/) and Vector Builder (vectorbuilder.com) free software. The plasmids were synthesized and assembled by Vector Builder. Plasmid DNA was purified using the Qiagen Maxi Prep kit (Qiagen Cat#10023). AAVs were also packaged by Vector Builder into AAV2/9. pENN.AAV.CamKII 0.4. Cre. SV40 (AAV5) (Addgene viral prep #105558-AAV5; http://n2t.net/addgene:105558; RRID:Addgene_105558), pAAV-CAG-TdTomato (AAV5) (Addgene viral prep#59462-AAV5; http://n2t.net/addgene:59462; RRID:Addgene_59462) and pCAG-FLEX-EGFP-WPRE (AAV9) (Addgene viral prep #51502-AAV9; http://n2t.net/addgene:51502; RRID:Addgene_51502) were obtained from Addgene (Oh, S.W., Harris, J.A., Ng, L., et al., 2014). rAAV5/AAV-EF1α-FlpO-WPRE and rAAV9/CAG-GFP were obtained from the UNC GTC Vector Core.

In utero electroporation. Pregnant ICR mice at E15.5 were anesthetized with isoflurane and an abdominal incision was made to expose the uterus. Pups were visualized through the uterine wall. Plasmids diluted in fast green and phosphate buffered saline (PBS) (3 µg/µl) were injected through sharpened glass capillary needles into the lateral ventricle. 5mm paddles were used to deliver five 40V pulses of 50ms each with 950ms intervals across the hemispheres. Uterine horns were repositioned inside the female and the abdominal cavity was filled with 5x penicillin/streptomycin (pen/strep) in sterile PBS. Pups were collected at E17.5 via transcardial perfusion with PBS and 4% paraformaldehyde (PFA) and fixed in 4% PFA for four hours at 4°C, rinsed with PBS, and sectioned coronally at 150um on a vibrating microtome (VT100S; Leica). Immunohistochemistry was performed as described (Polleux & Ghosh, 2002). Nuclei were visualized with DAPI (10g/ml) and primary antibodies used were chicken anti-GFP (1:500, Aves Labs Cat# GFP-1010) and rabbit anti-dsRed (1:500, Takara Bio Cat# 632475) with secondary antibodies goat anti-chicken 488 (1:1000, Thermo Fisher Scientific Cat# A-11039) and goat anti-rabbit 546 (1:1000, Abcam Cat# ab60317). Sections were mounted on glass microscope slides with Fluoro Gel (Electron Microscopy Sciences Cat# 1798502) and imaged with a laser-scanning confocal microscope (Leica SPEII).

***Ex utero* electroporation.** *Ex utero* electroporation was performed similarly as *in utero* electroporation. Pregnant ICR mice at E14.5 were cervically dislocated, uterine horns were removed, and pups were dissected out in Complete HBSS on ice. Plasmids were injected bilaterally and 5mm paddles were used to deliver five 40V pulses of 50ms each

with 950 ms intervals across each hemisphere. After electroporation, cortices were removed for primary cortical culture.

Primary Cortical Neuron Culture. Primary cortical neurons were isolated from E14.5 ICR mouse embryos as described (Kim & Magrané, 2011) using growth media as described (Polleux and Ghosh 2010). 12mm circular coverslips were treated with 12M HCL overnight and thoroughly neutralized with deionized water. Acid-treated coverslips were stored in a glass petri dish with 70% to 100% Ethanol. The coverslips were fire-sterilized prior to use and coated with laminin and poly-D-lysine (8.3ug/mL) in sterile water in a 24-well sterile culture plate. *Ex utero* electroporation was performed prior to dissection in Complete Hanks Balanced Salt Solution (HBSS, 2.5mM HEPES pH7.4, 2.5mM D-glucose, 1mM $CaCl_2$, 1mM $MgSO_4$, 2.5mM $NaHCO_3$). Neurons were plated at a density of $2.6x10^5$cells/cm^2 and maintained in Complete Neurobasal (Neurobasal media, pen/strep, Glutamax, B27) in 5% CO_2 at 37°C. 50% of the media was exchanged with fresh media 48 hours after plating. Neurons were collected after 72 hours and fixed in 4% PFA for 5 minutes, then rinsed with PBS 3x for 5 min. Cells were incubated in blocking buffer (PBS, 1% goat or donkey serum, 0.1% Triton-X) for 30 minutes at RT, rinsed with PBS 1x, then incubated in primary antibodies (chicken anti-GFP (1:1000, Aves Labs Cat# GFP-1010) and/or rabbit anti-dsRed (1:1000, Takara Bio Cat# 632475) in antibody dilution buffer (PBS, 0.1% goat or donkey serum) at 4°C overnight. The following day cells were rinsed in PBS 4x for 5min, and were incubated in secondary antibodies (goat anti-chicken 488 (1:1000, Thermo Fisher Scientific Cat# A-11039) and goat anti-rabbit 546 (1:1000, Abcam Cat# ab60317)) and DAPI (1ug/mL)

in antibody dilution buffer for 2 hours, then rinsed with PBS 4x for 10min. Coverslips were mounted on glass slides with Fluoro Gel and imaged with a confocal microscope.

Neuro2A Cell Culture. Neuro2A (N2A) cells from ATCC were maintained in DMEM with pen/strep and 10% fetal bovine serum and incubated in 5% CO_2 at 37°C. Cells were plated on laminin and poly-D-lysine (8.3µg/ml) coated 12mm coverslips in a 24-well plate at $7.8x10^4$cells/cm^2. Cells were transfected 24 hours later with Metafectene PRO (Biontex Cat# T040-1.0) according to manufacturer's suggested protocol with a 1:4 DNA to Metafectene ratio. Cells were fixed 48 hours after transfection with 4% PFA for 5 min, rinsed with PBS, stained with DAPI (1 µm/mL) for one hour, then rinsed again with PBS 3x for 5min. Coverslips were mounted with Fluoro Gel onto a glass slide and examined with confocal microscopy.

Stereotaxic Injections. Stereotaxic injections were performed as described previously (Osten et al., 2007) in P30 mice. Mice were put under anesthesia for the duration of the procedure using isoflurane. Injections for AAV-FlpOn-CreOff-TdTomato expression experiments were performed in CD1 mice targeting the DG of the Hippocampus (coordinates: A/P -1.70 mm; M/L ±1.90 mm; D/V, -1.70 mm). Right hemisphere injections received a 400nl viral cocktail of AAV-FlpOn-CreOff-TdTomato ($6.55x10^{12}$ GC/mL), rAAV5/EF1α-FlpO-WPRE, pENN.AAV.CamKII 0.4. Cre. SV40, and pCAG-FLEX-EGFP-WPRE in a 1:1:1:1 ratio, whereas the contralateral hemisphere received a 200nl viral cocktail containing FlpOn-CreOff-TdTomato ($6.55x10^{12}$ GC/mL), EF1α-FlpO-WPRE, in a 1:1 ratio. Titers for commercially available AAVs were as follows: pENN.AAV.CamKII 0.4. Cre. SV40 (2.4 x 10^{13} GC/ml), pCAG-FLEX-EGFP-WPRE (3.3 x 10^{13} GC/ml), pAAV-CAG-TdTomato (1.2 x 10^{13} GC/ml), rAAV5/EF1α-FlpO-WPRE (2.6

x 10^{12} GC/ml), and rAAV9/CAG-GFP (2 x 10^{12} GC/ml). FlpO-negative controls were injected with a viral cocktail of FlpOn-CreOff-TdTomato and pAAV-CAG-GFP. For viral CreOn-FlpOff-EGFP construct experiments, injections were performed in *Grik4-Cre* mice. Right hemisphere injections received 200nl of desired CreOn-FlpOff construct, whereas the contralateral left hemisphere received a 500nl viral cocktail containing the construct, rAAV5/EF1α-FlpO-WPRE, and pAAV-CAG-TdTomato in a 2:2:1 ratio (respectively). Viral CreOn-FlpOff-EGFP constructs co-expressing following GOIs were tested: Kir2.1 (3.34x10^{13} GC/ml), Kir2.1-mutant (4.6x10^{13} GC/ml), NaChBac (2.98x10^{12} GC/ml), NaChBac-mutant (4.93x10^{13} GC/ml), and TeTN (2.52x10^{12} GC/ml). Three weeks after injections, mice were perfused and fixed with 4% paraformaldehyde O/N at 4 °C, rinsed in PBS x1, and sectioned coronally on a vibratome (150 µm). Sections were incubated in 4',6-diamidino-2-phenylindole (DAPI) and mounted onto slides with Fluoro Gel fluorescence mounting medium (Electron Microscopy Sciences Cat# 1798502). Expression was observed via confocal microscopy.

Image analysis. N2A and primary cortical neuron image analysis was performed with FIJI (Schindelin et al., 2012). GFP+ and RFP+ cells were all manually counted. DAPI counts were obtained by thresholding the DAPI channel, image was made binary, then the watershed function was used and finally the analyze particles function to count nuclei with a size between 20-2000 pixels^2 and 0.2-1.0 circularity. Transfection efficiency was calculated as $\frac{\#RFP\ or\ \#GFP}{\#DAPI} \times 100$. Percentage of transfected cells in which recombinase activity resulted in fluorescent reporter (RFP or GFP) expression were calculated as $\frac{\#GFP\ or\ RFP}{\#\ transfected} \times 100$. Images obtained from *in utero* electroporations were counted manually, avoiding the ventricular zone where it became impossible to

distinguish individual cells. Percentage of ON cells were calculated the same as in N2A and primary cortical neurons. The N2A, primary cortical culture, and intrauterine electroporation datasets were tested for normality with the Shapiro-Wilk test and QQ plot. A One-way ANOVA with Tukey's multiple comparisons test was done for N2A transfection and intrauterine electroporation data (Figures 1,2,4). Unpaired t-test was performed on viral injection data (Figures S1 and S3). The data set for primary cortical cell counts failed to meet normality and thus Fisher's exact test was performed (Figure 3). Image analysis for viral constructs was performed with ImageJ. A region of interest in granule cell layer of the DG and defined by the site of injection was selected. Mean pixel intensity of the viral reporter fluorophore in the ROI was measured. An uninjected region of the hippocampus was simultaneously selected and measured for fluorescence intensity, and defined as background fluorescence. Background fluorescence was then subtracted from the mean pixel intensity of the ROI. The percentage of viral reporter expression maintained when the OFF recombinase was co-injected was calculated as $\frac{mean\ pixel\ intensity\ OFF}{mean\ pixel\ intensity\ ON} \times 100$ for each animal, and was averaged across samples (n=3) for each viral construct.

Acknowledgements

We would like to thank Drs. Edward Zagha and Kevin Wright for critically reading the manuscript and providing helpful comments. We would like to thank the University of North Carolina Chapel Hill Gene Therapy Center Vector Core for packaging of viral constructs. pENN.AAV.CamKII 0.4.Cre.SV40 was a gift from James M. Wilson, pCAG-

FLEX-EGFP-WPRE was a gift from Hongkui Zeng, and pAAV-CAG-TdTomato and pAAV-CAG-GFP were a gift from Edward Boyden. AAV-EF1α-FlpO-WPRE was a gift from Karl Deisseroth.

Competing interests

The authors declare no competing financial interests.

Funding sources

This work was supported by grants from the National Institutes of Health (R21MH118640 and R01NS104026 to M.M.R.; R01NS069861 and R01NS097750 to V.S) and a Hellman Foundation Fellowship to M.M.R.

References

(Bolded names = Co-first authorship)

Antón-bolaños, N., Sempere-ferràndez, A., Guillamón-Vivancos, T., Martini, F. J., Pérez-Saiz, L., Gezelius, H., Filipehuk, A., Valdeolmillos, M., López-Bendito, G. (2019). Prenatal activity from thalamic neurons governs the emergence of functional cortical maps in mice. *Science*, 364(6444), 987–990. https://doi.org/10.1126/science.aav7617

Atasoy, D., Aponte, Y., Su, H. H., & Sternson, S. M. (2008). A FLEX Switch Targets Channelrhodopsin-2 to Multiple Cell Types for Imaging and Long-Range Circuit Mapping. *Journal of Neuroscience*, *28*(28), 7025–7030. https://doi.org/10.1523/JNEUROSCI.1954-08.2008

Awatramani, R., Soriano, P., Rodriguez, C., Mai, J. J., & Dymecki, S. M. (2003). Cryptic boundaries in roof plate and choroid plexus identified by intersectional gene activation, *Nat. Genet.*, *35*(1), 70–75. https://doi.org/10.1038/ng1228

Bando, Y., Irie, K., Shimomura, T., Umeshima, H., Kushida, Y., Kengaku, M., Fujiyoshi, Y., Hirano, T., Tagawa, Y. (2016). Control of Spontaneous Ca2+ Transients Is Critical for Neuronal Maturation in the Developing Neocortex. Cerebral Cortex, 26(1), 106–117. https://doi.org/10.1093/cercor/bhu180

Branda, C. S., & Dymecki, S. M. (2004). Talking about a Revolution: The Impact of Site-Specific Recombinases on Genetic Analyses in Mice. *Developmental Cell*, *6*, 7–28.

Burrone, J., O'Byrne, M., & Murthy, V. N. (2002). Multiple forms of synaptic plasticity triggered by selective suppression of activity in individual neurons. *Nature*, 420(6914), 414–418. https://doi.org/10.1038/nature01242

Capecchi, M. (1989). Altering the genome by homologous recombination. *Science*, *244*(4910), 1288–1292. https://doi.org/10.1126/science.2660260

Che, A., Babij, R., Iannone, A. F., Fetcho, R. N., Ferrer, M., Liston, C., Fishell, G., De Marco Garcia, N. V. (2018). Layer I interneurons sharpen sensory maps during neonatal development. *Neuron*, 99(1), 98–116. https://doi.org/10.1016/j.neuron.2018.06.002.Layer

Daigle, T. L., Madisen, L., Hage, T. A., Valley, M. T., Knoblich, U., Larsen, R. S., … Li, L. (2019). A suite of transgenic driver and reporter mouse lines with enhanced brain cell type targeting and functionality. *Cell*, 174(2), 465–480. https://doi.org/10.1016/j.cell.2018.06.035.A

Darmanis, S., Sloan, S. A., Zhang, Y., Enge, M., Caneda, C., Shuer, L. M., Hayden Gephart, M. G., Barres, B. A., & Quake, S. R. (2015). A survey of human brain transcriptome diversity at the single cell level. *Proceedings of the National Academy of Sciences*, 112(23), 7285–7290. https://doi.org/10.1073/pnas.1507125112

Dong, J., Fan, P., & Frizzell, R. A. (1996). Quantitative analysis of Packaging Capacity of Recombinant Adeno-Associated Virus. *Human Gene Therapy*, 7, 2101–2112.

Dymecki, S. M., Ray, R. S., & Kim, J. C. (2010). Mapping Cell Fate and Function Using Recombinase-Based Intersectional Strategies. Guide to Techniques in Mouse Development, Part B: Mouse Molecular Genetics*. Methods Enzymol.* (2nd ed., Vol. 477). https://doi.org/10.1016/S0076-6879(10)77011-7

Fenno, L. E., Mattis, J., Ramakrishnan, C., Hyun, M., Lee, S. Y., He, Tucciarone, J., Selimbeyoglu, A., Berndt, A., Grosenick, L., Zalocusky, K.A., Bernstein, H., Swanson, H., Perry, C., Diester, I., Boyce, F.M., Bass, C., Neve, R., Huang, Z.J., & Deisseroth, K. (2014). Targeting cells with single vectors using multiple-feature Boolean logic. *Nature Methods, 11*, 763–772. https://doi.org/10.1038/nmeth.2996

Garcıa-Garcia, M. J., Eggenschwiler, J. T., Caspary, T., Alcorn, H. L., Wyler, M. R., Huangfu, D., Rakeman, A.S., Lee, J.D., Feinberg, E.H., Timmer, J.R., & Anderson, K. V. (2005). Analysis of mouse embryonic patterning and morphogenesis by forward genetics. *PNAS*, *5*(7), 5913–5919. www.pnas.org/cgi/doi/10.1073/pnas.0501071102

Gerfen, C. R., Paletzki, R., & Heintz, N. (2013). GENSAT BAC cre-recombinase driver lines to study the functional organization of cerebral cortical and basal ganglia circuits. *Neuron*, 80(6), 1368–1383. https://doi.org/10.1016/j.neuron.2013.10.016

Glover, C. P., Bienemann, A. S., Heywood, D. J., Cosgrave, A. S., & Uney, J. B. (2002). Adenoviral-mediated, high-level, cell-specific transgene expression: a SYN1-WPRE cassette mediates increased transgene expression with no loss of neuron specificity. *Molecular therapy: the journal of the American Society of Gene Therapy*, *5*(5 Pt 1), 509–516. https://doi.org/10.1006/mthe.2002.0588

Goodrich, M. M., Talhouk, R., Zhang, X., & Goodrich, D. W. (2018). An approach for controlling the timing and order of engineered mutations in mice. *Genesis* (New York, N.Y. : 2000), 56(8), e23243. https://doi.org/10.1002/dvg.23243

Gordon, J., & Ruddle, F. (1981). Integration and stable germ line transmission of genes injected into mouse pronuclei. *Science*, 214(4526), 1244–1246. https://doi.org/10.1126/science.6272397

Gradinaru, V., Zhang, F., Ramakrishnan, C., Mattis, J., Prakash, R., Diester, I., Goshen, I., Thompson, K. R., Deisseroth, K. (2010). Molecular and Cellular Approaches for Diversifying and Extending Optogenetics. *Cell*, *141*(1), 154–165. https://doi.org/10.1016/j.cell.2010.02.037

Gu, H., Marth, J. D., Orban, P. C., Mosmann, H., & Rajewsky, K. (1994). Deletion of a DNA Polymerase β Gene Segment in T Cells Using Cell Type-Specific Gene Targeting. *Science*, 265(5168), 103–106. https://doi.org/10.1126/science.8016642

He, M., Tucciarone, J., Lee, S., Nigro, M. J., Kim, Y., Levine, J. M., Kelly, S.M., Krugikov, I., Wu, P., Chen, Y., Gong, L., Hou, Y., Osten, P., Rudy, B., Huang, Z. J.

(2016). *Neuron*, 91(6), 1228–1243. https://doi.org/10.1016/j.neuron.2016.08.021.Strategies

Hogan, B., & Williams, J. (1981). Integration of foreign genes into the mammalian germ line: Genetic engineering enters a new era. *Nature*, 294(5836), 9–10. https://doi.org/10.1038/294009a0

Jaenisch, R., & Mintz, B. (1974). Simian Virus 40 DNA Sequences in DNA of Healthy Adult Mice Derived from Preimplantation Blastocysts Injected with Viral DNA. *Proceedings of the National Academy of Sciences*, 71(4), 1250–1254. https://doi.org/10.1073/pnas.71.4.1250

Jensen, P., & Dymecki, S. M. (2014). Essentials of Recombinase-Based Genetic Fate Mapping in Mice. *Methods Mol Biol*, *1092*, 437–454. https://doi.org/10.1007/978-1-60327-292-6

Johns, D. C., Marx, R., Mains, R. E., O'Rourke, B., & Marbán, E. (1999). Inducible genetic suppression of neuronal excitability. *Journal of Neuroscience*, 19(5), 1691–1697. https://doi.org/10.1523/jneurosci.19-05-01691.1999

Kakava-georgiadou, N., Zwartkruis, M. M., Bullich-vilarrubias, C., Adan, R. A. H., & Marti, F. (2019). An Intersectional Approach to Target Neural Circuits With Cell- and Projection-Type Specificity: Validation in the Mesolimbic Dopamine System. *Frontiers in Molecular Neuroscience*, *12*(February), 1–9. https://doi.org/10.3389/fnmol.2019.00049

Kim H.J., Magrané J. (2011) Isolation and Culture of Neurons and Astrocytes from the Mouse Brain Cortex. In: Manfredi G., Kawamata H. (eds) Neurodegeneration. Methods in Molecular Biology (Methods and Protocols), vol 793. Humana Press, Totowa, NJ

Kozorovitskiy, Y., Saunders, A., Johnson, C. A., Lowell, B. B., Sabatini, B. L., Israel, B., & Medical, D. (2012). Recurrent network activity drives striatal synaptogenesis. *Nature*, *485*(7400), 646–650. https://doi.org/10.1038/nature11052.

Kristianto, J., Johnson, M. G., Zastrow, R. K., Radcliff, A. B., & Blank, R. D. (2017). Spontaneous recombinase activity of Cre-ERT2 in vivo. *Transgenic research*, 26(3), 411–417. https://doi.org/10.1007/s11248-017-0018-1

Lin, C. W., Sim, S., Ainsworth, A., Okada, M., Kelsch, W., & Lois, C. (2010). Genetically Increased Cell-Intrinsic Excitability Enhances Neuronal Integration into Adult Brain Circuits. *Neuron*, 65(1), 32–39. https://doi.org/10.1016/j.neuron.2009.12.001

Madisen, L., Garner, A. R., Carandini, M., Zeng, H., & Cheng, A. (2015). Transgenic Mice for Intersectional Targeting of Neural Sensors and Effectors with High Specificity and Performance. *Neuron, 85*, 942–958. https://doi.org/10.1016/j.neuron.2015.02.022

Merte, J., Wang, Q., Vander Kooi, C. W., Sarsfield, S., Leahy, D. J., Kolodkin, A. L., & Ginty, D. D. (2010). A forward genetic screen in mice identifies Sema3A^{K108N}, which

binds to Neuropilin-1 but cannot signal. *Journal of Neuroscience*, *30*(16), 5767-5775. https://doi.org/10.1523/JNEUROSCI.5061-09.2010

Nakazawa K; Quirk MC; Chitwood RA; Watanabe M; Yeckel MF; Sun LD; Kato A; Carr CA; Johnston D; Wilson MA; Tonegawa S. (2002). Requirement for hippocampal CA3 NMDA receptors in associative memory recall. Science 297(5579):211-8.

Nusslein-Volhard, C., & Wieschaus, E. (1980). Mutations affecting segment number and polarity in Drosophila. *Nature*, *287*(October), 795–801. https://doi.org/10.1038/287795a0

Oh, S. W., Harris, J. A., Ng, L., Winslow, B., Cain, N., Mihalas, S., Wang, Q., Lau, C., Kuan, L., Henry, A. M., Mortrud, M. T., Ouellette, B., Nguyen, T., Sorensen, S. A., Slaughterbeck, C., Wakeman, W., Li, Y., Feng, D., … Anh Zeng, H. (2014). A mesoscale connectome of the mouse brain. Nature, 508(7495), 207–214. https://doi.org/10.1038/nature13186 Okada, M., & Matsuda, H. (2008). Chronic lentiviral expression of inwardly rectifying K+ channels (Kir2.1) reduces neuronal activity and downregulates voltage-gated potassium currents in hippocampus. *Neuroscience*, 156(2), 289–297. https://doi.org/10.1016/j.neuroscience.2008.07.038

Osten, P., Cetin, A., Komai, S., Eliava, M., & Seeburg, P. H. (2007). Stereotaxic gene delivery in the rodent brain. *Nature Protocols*, 1(6), 3166–3173.

Plummer, N. W., Evsyukova, I. Y., Robertson, S. D., Marchena, J. De, Tucker, C. J., & Jensen, P. (2015). Expanding the power of recombinase-based labeling to uncover cellular diversity. *Development, 142*, 4385–4393. https://doi.org/10.1242/dev.129981

Polleux, F., & Ghosh, A. (2002). The Slice Overlay Assay: A Versatile Tool to Study the Influence of Extracellular Signals on Neuronal Development. *Science's STKE*, 2002(136), pl9.

Priya, R., Paredes, M. F., Karayannis, T., Yusuf, N., Liu, X., Jaglin, X., Graef, I., Alvarez-Buylla A., Fishell, G. (2018). Activity Regulates Cell Death within Cortical Interneurons through a Calcineurin-Dependent Mechanism. *Cell Reports*, 22(7), 1695–1709. https://doi.org/10.1016/j.celrep.2018.01.007

Rubin, G., & Spradling, A. (1982). Genetic transformation of Drosophila with transposable element vectors. *Science*, *218*(4570), 348–353. https://doi.org/10.1126/science.6289436

Sauer, B., & Mcdermott, J. (2004). DNA recombination with a heterospecific Cre homolog identified from comparison of the pac-c1 regions of P1-related phages. *Nucleic Acids Research, 32*(20), 1–10. https://doi.org/10.1093/nar/gkh941 1–10 doi:10.1093/nar/gkh941

Saunders, A., Johnson, C. A., Sabatini, B. L., & Miyamichi, K. (2012). Novel recombinant adeno-associated viruses for Cre activated and inactivated transgene

expression in neurons. *Frontiers in Neural Circuits*, *6*(47), 1–10. https://doi.org/10.3389/fncir.2012.00047

Schindelin, J., Arganda-Carreras, I., Frise, E., Kaynig, V., Longair, M., Pietzsch, T., Preibisch, S., Rueden, C., Saalfeld, S., Schmid, B., Tinevez, J.-Y., White, D. J., Hartenstein, V., Eliceiri, K., Tomancak, P., & Cardona, A. (2012). Fiji: An open-source platform for biological-image analysis. *Nature Methods*, 9(7), 676–682.

Schnütgen, F., Doerflinger, N., Calléja, C., Wendling, O., Chambon, P., & Ghyselinck, N. B. (2003). A directional strategy for monitoring Cre-mediated recombination at the cellular level in the mouse. *Nature Biotechnology, 21*, 562–565. https://doi.org/10.1038/nbt811

Sim, S., Antolin, S., Lin, C. W., Lin, Y. X., & Lois, C. (2013). Increased cell-intrinsic excitability induces synaptic changes in new neurons in the adult dentate gyrus that require Npas4. *Journal of Neuroscience*, 33(18), 7928–7940. https://doi.org/10.1523/JNEUROSCI.1571-12.2013

Sternson, S. M., Atasoy, D., Betley, J. N., Henry, F. E., & Xu, S. (2016). An Emerging Technology Framework for the Neurobiology of Appetite. *Cell Metabolism*, *23*(2), 234–253. https://doi.org/10.1016/j.cmet.2015.12.002

Sweeney, S.T., Broadie, K., Keane, J., Niemann H., O'Kane, C.J. (1995). Targeted expression of tetanus toxin light chain in Drosophila specifically eliminates synaptic transmission and causes behavioral defects. *Neuron* 14, 341–351.

Tremblay, R., Lee, S., & Rudy, B. (2016). GABAergic Interneurons in the Neocortex: From Cellular Properties to Circuits. *Neuron*, 91(2), 260–292. https://doi.org/10.1016/j.neuron.2016.06.033

Tsien, J. Z., Chen, D. F., Gerber, D., Tom, C., Mercer, E. H., Anderson, D. J., Mayford, M., Kandel, E. R., & Tonegawa, S. (1996). Subregion- and Cell Type–Restricted Gene Knockout in Mouse Brain. *Cell*, 87(7), 1317–1326. https://doi.org/10.1016/S0092-8674(00)81826-7

Wright, K. M., Lyon, K., Leung, H., Leahy, D. J., Ma, L., & David, D. (2013). Dystroglycan organizes axon guidance cue localization and axonal pathfinding. *Neuron*, *76*(5), 931–944. https://doi.org/10.1016/j.neuron.2012.10.009.

Xue, M., Atallah, B. V., & Scanziani, M. (2014). Equalizing excitation-inhibition ratios across visual cortical neurons. *Nature*, *511*(7511), 596–600. https://doi.org/10.1038/nature13321

Zhang, F., Aravanis, A.M., Adamantidis, A., Lecea, L., and Deisseroth, K. (2007). Circuit-breakers: optical technologies for probing neural signals and systems. *Nature Reviews Neuroscience* 8(August), 577–581. https://doi:10.1038/nr n2192

Figure Legends

Table 1. Conceptual basis for the Expression by Boolean Exclusion (AND NOT) system using multiple recombinases. Expression of a gene of interest (GOI) can be spatially and temporally manipulated through the use of multiple recombinases. In this model, expression of a GOI depends on the presence of an ON recombinase, and is prevented by the presence of an OFF recombinase. Thus, gene expression only occurs in cells where the ON recombinase is present AND NOT the OFF recombinase. Controlling where and when the ON and OFF recombinases are expressed provides a high level of specificity for targeting cell populations.

Figure 1. Design and proof of concept for CreOn-FlpOff constructs. (A) Schematic representation of the CreOn-FlpOff construct. It is composed of an inverted expression cassette encoding for a coding sequence (CDS) fused to an HA tag, a P2A site, and EGFP, which is flanked by Frt, lox2722, and loxP sites. Presence of Cre recombinase results in inversion of the cassette and expression. Presence of FlpO results in removal of the cassette. **(B)** Expression of fluorescent reporter proteins in Neuro2A cells transfected with CreOn-FlpOff-EGFP construct (green) and pCAG-mCherry (red, loading control). Co-transfection with pCAG-Cre plasmid causes inversion of the cassette into the “ON” position and EGFP expression. Co-transfection of pCAG-FlpO deletes the cassette and abolishes EGFP expression. (B, right panel) Quantification of N2A cell transfections. Upon transfection with Cre, the CreOn-FlpOff-EGFP construct results in 93.9%±0.3 of transfected cells expressing EGFP, while co-transfection with FlpO results in abolishment of EGFP expression. N=3 independent experiments, error

bars ±SEM. ANOVA p<0.001; Tukey post-hoc test *** p<0.0001 vs. all other transfections. Scale bar 30μm.

Figure 2. Design and proof of principle for FlpOn-CreOff constructs. (A) Schematic representation of the FlpOn-CreOff construct. The inverted expression cassette is flanked by lox2722, F14, and Frt sites. Presence of Flp recombinase results in inversion of the cassette and expression. Presence of Cre results in removal of the cassette. **(B)** Expression of fluorescent reporters in Neuro2A cells transfected with FlpOn-CreOff-TdTomato construct (red) and pCAG-EGFP (green, transfection control) in Neuro2A cells. Co-transfection with pCAG-FlpO causes inversion of the cassette into the “ON” position and TdTomato expression. Transfection with pCAG-Cre removes the cassette and abolishes TdTomato expression. Upon transfection with FlpO, the FlpOn-CreOff-TdTomato construct results in detectable expression of reporter in 85.8%±5.6 of transfected cells, while co-transfection with Cre results in abolishment of TdTomato expression (right panel). N=3 independent experiments, error bars ±SEM. ANOVA p<0.01; Tukey post-hoc test *** p<0.0001 vs. all other transfections. Scale bar 30μm.

Figure 3. Validation of CreOn-FlpOff in primary cortical neurons. (A) Primary cortical neurons transfected with CreOn-FlpOff and Cre results in 100%±0.0 of transfected cells expressing EGFP. Without Cre or in the presence of FlpO there is no EGFP expression in any neurons. pCAG-mCherry was co-transfected as transfection control. **(B)** Primary cortical neurons transfected with FlpOn-CreOff-TdTomato and FlpO

results in detectable TdTomato expression in 92.1%±2.0 of transfected cells (right). pCAG-EGFP was co-transfected as transfection control. Without FlpO, or in the presence of Cre, there is no TdTomato expression in any neurons. N=3, error bars ±SEM. Fisher's exact test ***p<0.0001. Scale bar 30μm.

Figure 4. *In vivo* validation of CreOn-FlpOff and FlpOn-CreOff vectors via *in utero* electroporation (IUE). (A) Co-electroporation of CreOn-FlpOff-EGFP with mCherry reporter, Cre + pCAG-mCherry, FlpO-mCherry, or Cre + FlpO-mCherry in e15.5 ICR mouse embryos. Electroporation of CreOn-FlpOff-EGFP with Cre results in 97.7%±0.9 of transfected cells expressing EGFP (right). Electroporation with FlpO results in no expression and electroporation with Cre and FlpO results in only 1.7%±0.9 of cells still expressing EGFP. mCherry expression serves as electroporation control. **(B)** Co-electroporation of FlpOn-CreOff-TdTomato with pCAG-IRES-EGFP reporter, Cre-IRES-EGFP, FlpO, or Cre-IRES-EGFP + FlpO in e15.5 Swiss-Webster embryos. pCAG-IRES-EGFP expression was used as electroporation control.Electroporation of FlpOn-CreOff-TdTomato with FlpO results in 86.9%±3.1 of transfected cells expressing TdTomato (right). Co-electroporation with Cre, or with Cre and FlpO, results in no cells expressing TdTomato. N=3, error bars ±SEM. ANOVA p<0.001 for both sets of experiments; Tukey post-hoc test: *** p<0.0001 vs. all other transfections. Scale bar 100μm.

Figure 5. *In-vivo* validation of FlpOn-CreOff AAV by stereotactic injection in postnatal DG neurons. (A-I) Expression of viral FlpOn-CreOff-TdTomato construct

(red) in WT animals co-injected with pAAV-CAG-GFP **(A, D, G)**, with AAV-EF1α-FlpO-WPRE **(B, E, H),** or AAV-EF1α-FlpO-WPRE + AAV-CamKII-Cre + AAV-CAG-FLEX-EGFP **(C, F, I)**. EGFP expression is used to visualize the injection site in the absence of TdTomato expression. Even in the presence of FlpO, Cre injection resulted in inactivation of TdTomato reporter expression (**C**, **F**). DAPI (blue) was used to visualize nuclei. Scale bar: 150 μm.

Figure 6. In-vivo validation of CreOn-FlpOff AAV in the dentate gyrus of postnatal mice. (A-I) Expression of viral CreOn-FlpOff-EGFP construct (green) in WT animals (A, D, G), in Grik4-Cre animals (B, E, H), and in Grik4-Cre mice co-injected with AAV-EF1α-FlpO-WPRE (C, F, I). pAAV-CAG-TdTomato (red) was co-injected when necessary to visualize the injection site. Even in the presence of Cre, FlpO injection resulted in inactivation of reporter expression by the CreOn-FlpOff-EGFP virus (C, F). EGFP labeling in the molecular layer of AAV-EF1α-FlpO injected animals (C,F) is from axonal projections from the contralateral side. DAPI (blue) was used to visualize nuclei. Scale bar: 150 μm.

Figure 7. *In-vivo* validation of CreOn-FlpOff AAV constructs to manipulate neuronal activity. (A-T) Expression of fluorescent reporter by CreOn-FlpOff AAVs (green) co-expressing (A-D) Kir2.1, (E-H) Kir2.1-Mutant, (I-L) NaChBac, (M-P) NaChBac-mutant, and **(Q-T)** TETN in WT (A, E, I, M, Q) , *Grik4-Cre* animals **(B, F, J, N, R)** and *Grik4-Cre* animals co-injected with AAV-EF1α-FlpO-WPRE (C, D, G, H, K, L,

O, P, S, T). Injections delivering AAV-EF1α-FlpO included pAAV-CAG-TdTomato (red) in order to visualize infected cells. In the presence of Cre and FlpO, expression of the CreOn-FlpOff virus was inactivated (C, D, G, H, K, L, O, P, S, T). EGFP labeling in the molecular layer of TeTN/FlpO injected animals (T) is from axonal projections from the contralateral side. Scale bar: 150 μm.

Figure 8. The ExBoX system can be utilized in multiple ways. (A) Expression of a gene of interest (GOI) can be restricted to a specific subpopulation of cells. Only the subpopulation of cells expressing the ON recombinase, but not the OFF recombinase, will express the GOI. **(B)** ExBoX can also be used for temporal control of expression. In this scheme, activation of the ON recombinase is used just prior to a critical period of interest. Introduction or activation of the OFF recombinase at the end of this critical period will turn off expression of the GOI. This serves to reduce confounding factors during later experimental observation, as GOI expression is no longer present.

	No Recombinase	Cre Only	FlpO Only	Cre and FlpO
Cre = ON **FlpO = OFF**	○○○ ○○○ ○○○	●●● ●●● ●●●	○○○ ○○○ ○○○	○○○ ○○○ ○○○
FlpO = ON **Cre = OFF**	○○○ ○○○ ○○○	○○○ ○○○ ○○○	●●● ●●● ●●●	○○○ ○○○ ○○○

Table 1. Conceptual basis for the Expression by Boolean Exclusion (AND NOT) system using multiple recombinases.

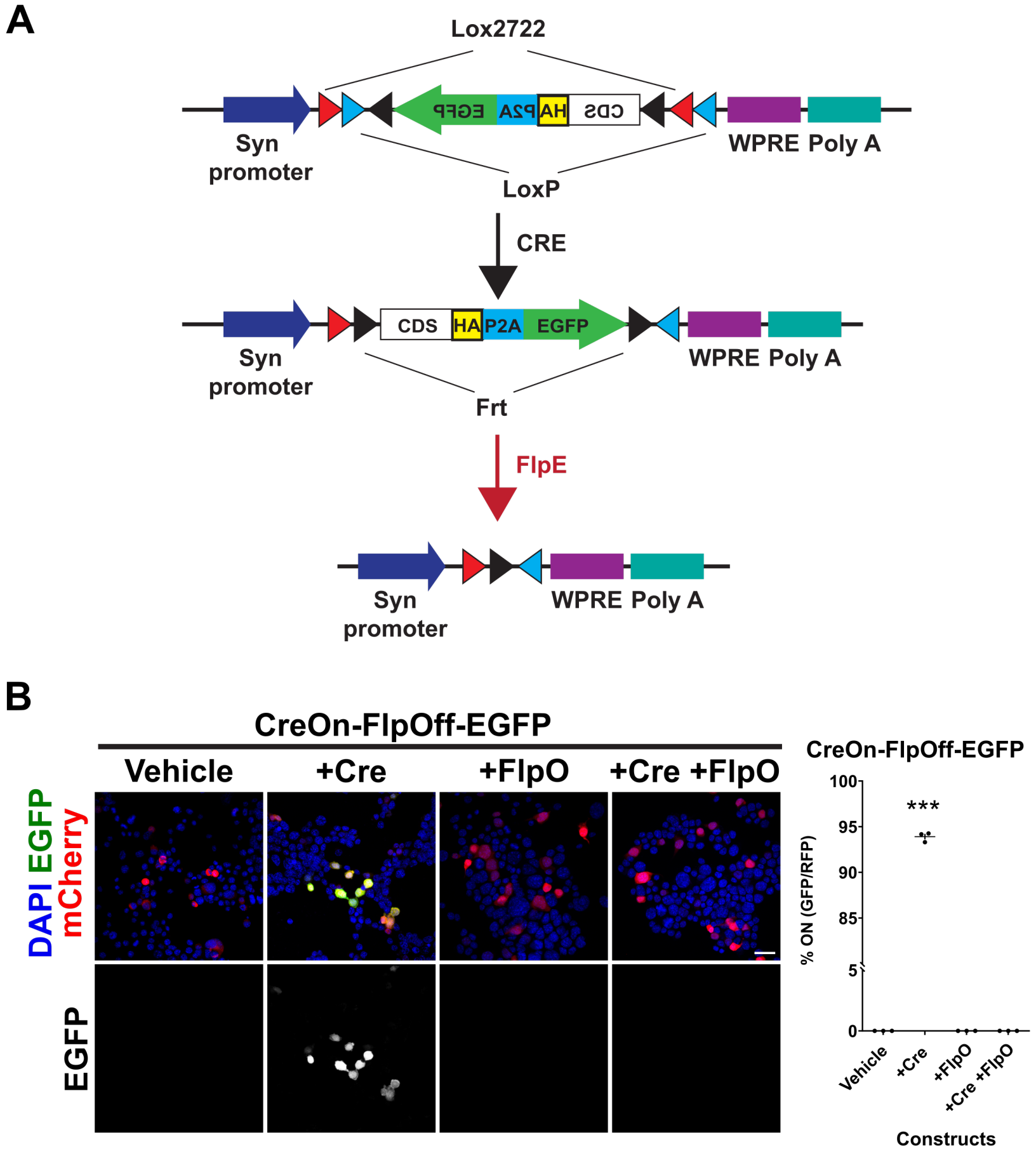
A
Lox2722
Syn promoter
WPRE Poly A
LoxP
CRE
CDS
HA
P2A
EGFP
Frt
FlpE
B
CreOn-FlpOff-EGFP
Vehicle
+Cre
+FlpO
+Cre +FlpO
DAPI EGFP mCherry
EGFP
% ON (GFP/RFP)
100
95
90
85
5
0
***
Constructs

Fig1

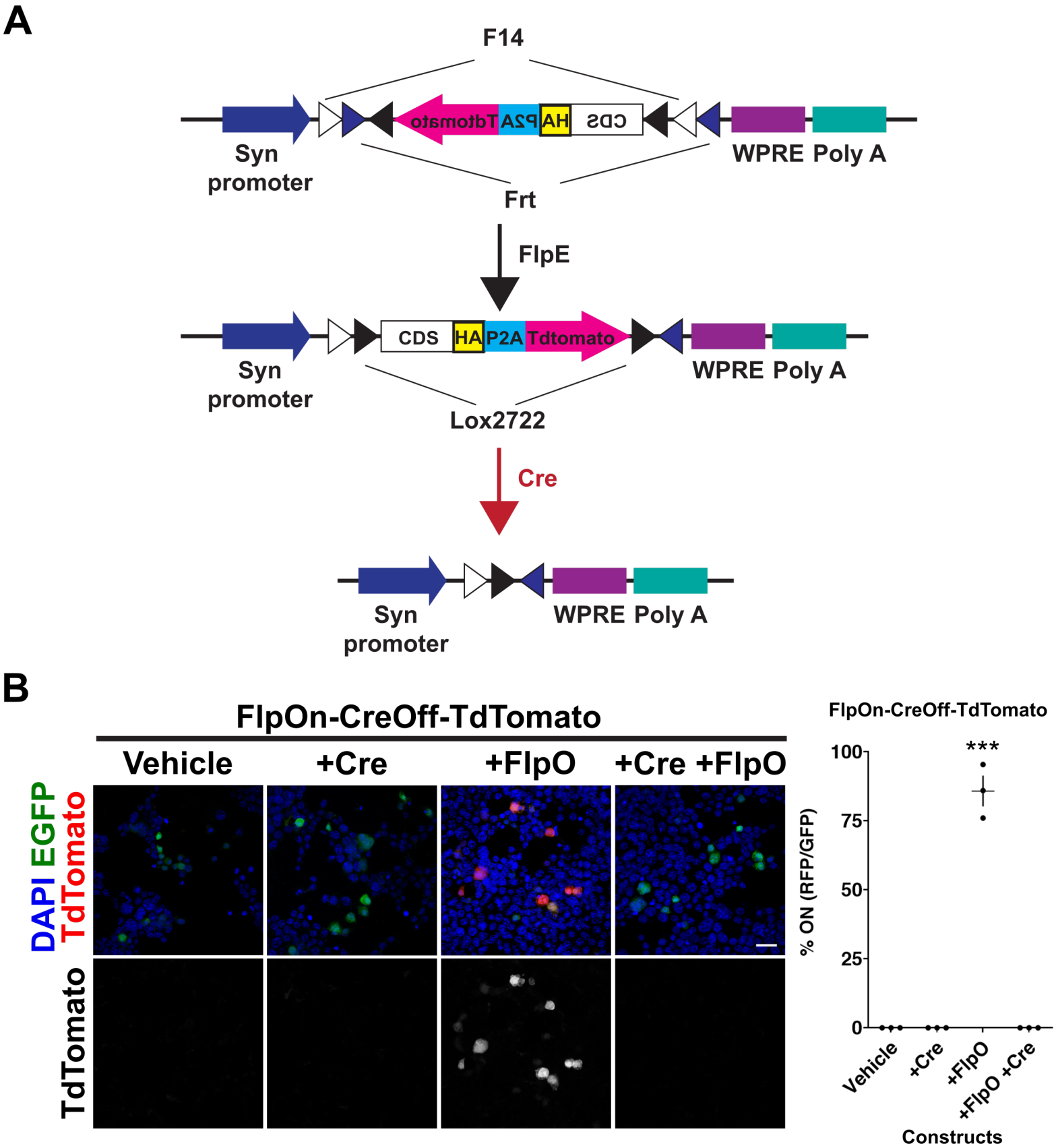
A
F14
Syn promoter
WPRE Poly A
Frt
FlpE
CDS
HA
P2A
Tdtomato
Syn promoter
WPRE Poly A
Lox2722
Cre
Syn promoter
WPRE Poly A
B
FlpOn-CreOff-TdTomato
Vehicle
+Cre
+FlpO
+Cre +FlpO
DAPI EGFP
TdTomato
TdTomato
FlpOn-CreOff-TdTomato
***
% ON (RFP/GFP)
100
75
50
25
0
Vehicle
+Cre
+FlpO
+FlpO +Cre
Constructs

Fig2

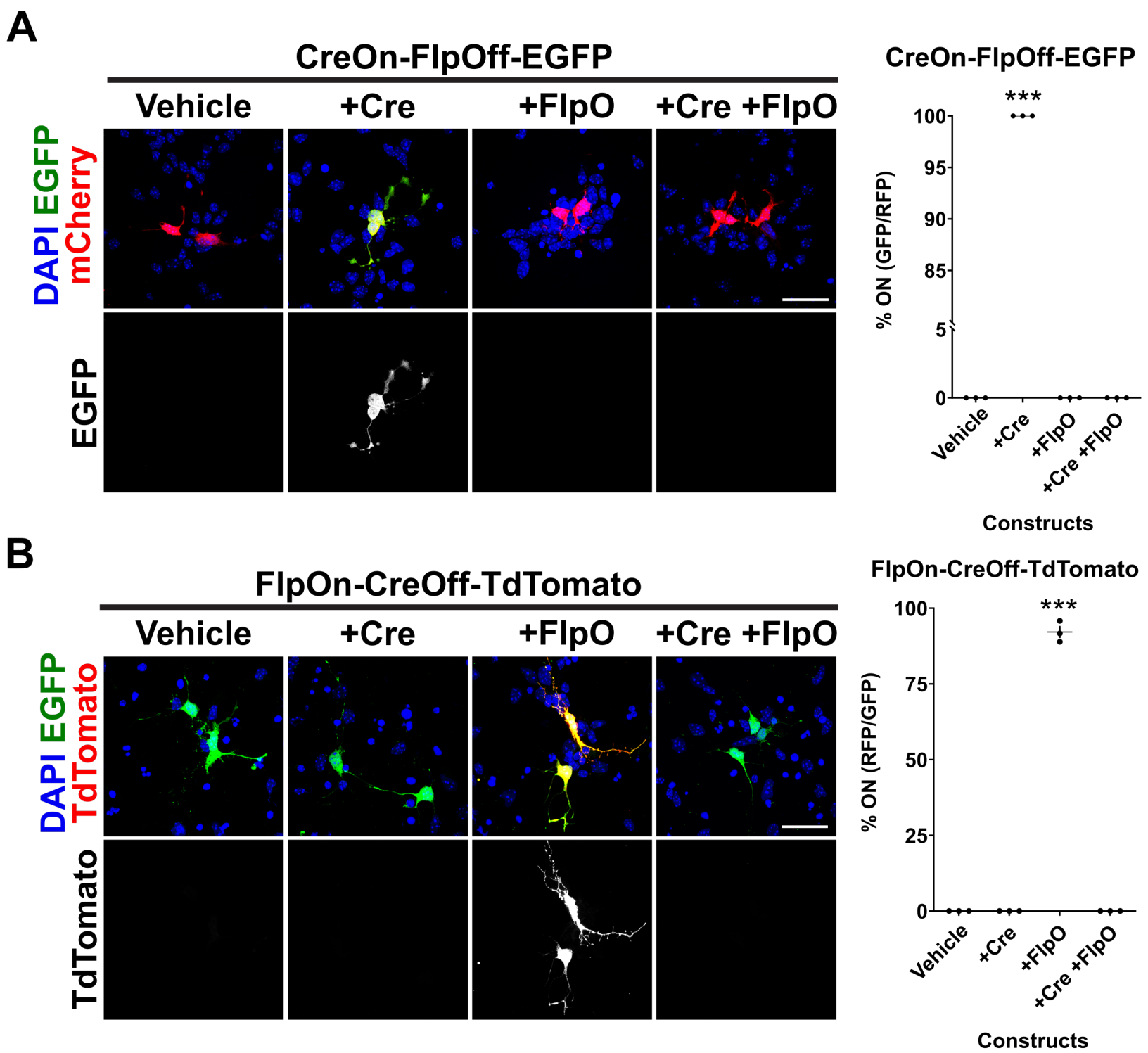
A
CreOn-FlpOff-EGFP
Vehicle
+Cre
+FlpO
+Cre +FlpO
DAPI EGFP
mCherry
EGFP
CreOn-FlpOff-EGFP
***
% ON (GFP/RFP)
100
95
90
85
5
0
Vehicle
+Cre
+FlpO
+Cre +FlpO
Constructs
B
FlpOn-CreOff-TdTomato
Vehicle
+Cre
+FlpO
+Cre +FlpO
DAPI EGFP
TdTomato
TdTomato
FlpOn-CreOff-TdTomato
***
% ON (RFP/GFP)
100
75
50
25
0
Vehicle
+Cre
+FlpO
+Cre +FlpO
Constructs

Fig3

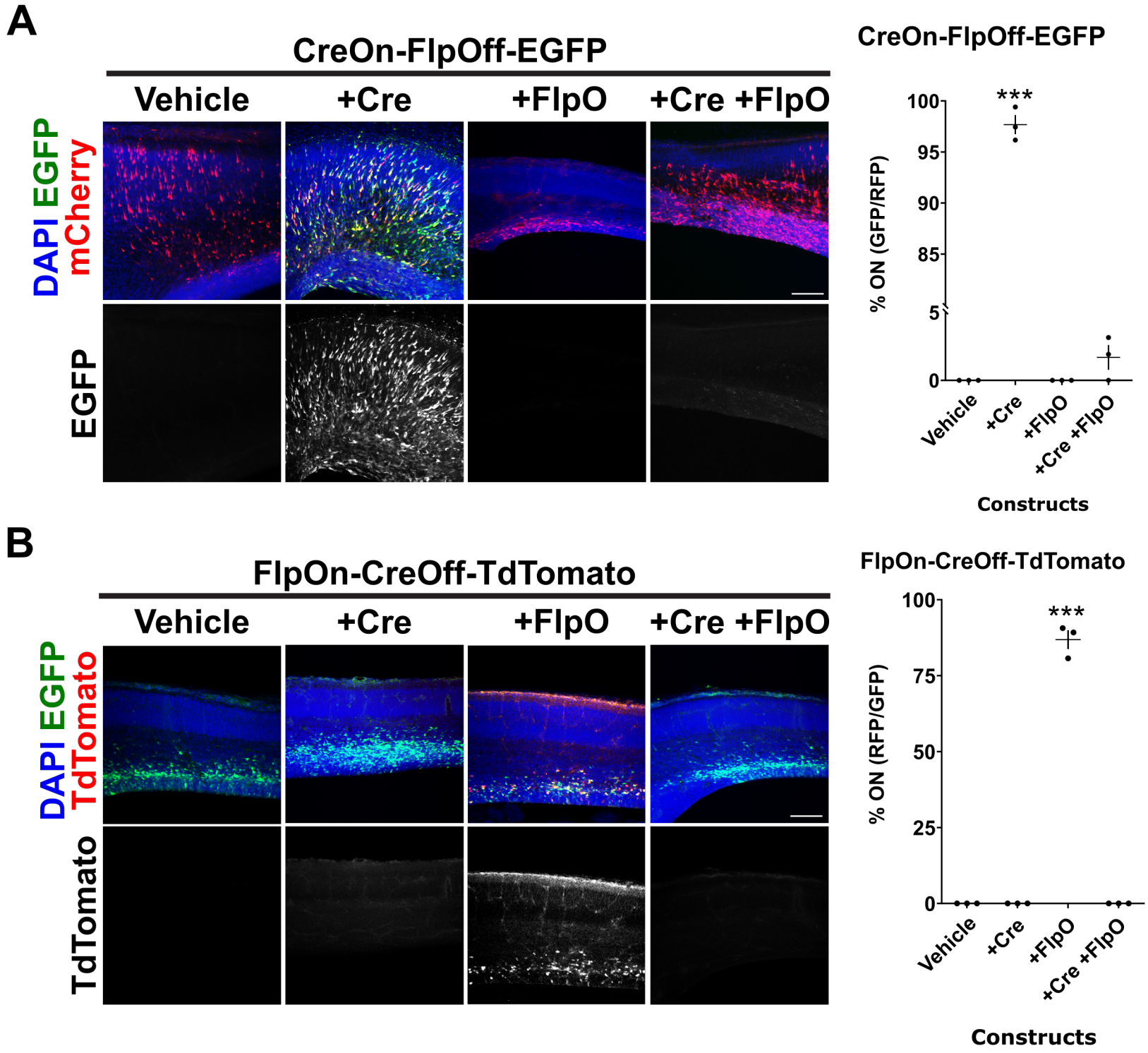
A
CreOn-FlpOff-EGFP
Vehicle
+Cre
+FlpO
+Cre +FlpO
DAPI EGFP
mCherry
EGFP
CreOn-FlpOff-EGFP
% ON (GFP/RFP)
100
95
90
85
5
0
***
Vehicle
+Cre
+FlpO
+Cre +FlpO
Constructs
B
FlpOn-CreOff-TdTomato
Vehicle
+Cre
+FlpO
+Cre +FlpO
DAPI EGFP
TdTomato
TdTomato
FlpOn-CreOff-TdTomato
% ON (RFP/GFP)
100
75
50
25
0
***
Vehicle
+Cre
+FlpO
+Cre +FlpO
Constructs

Fig4

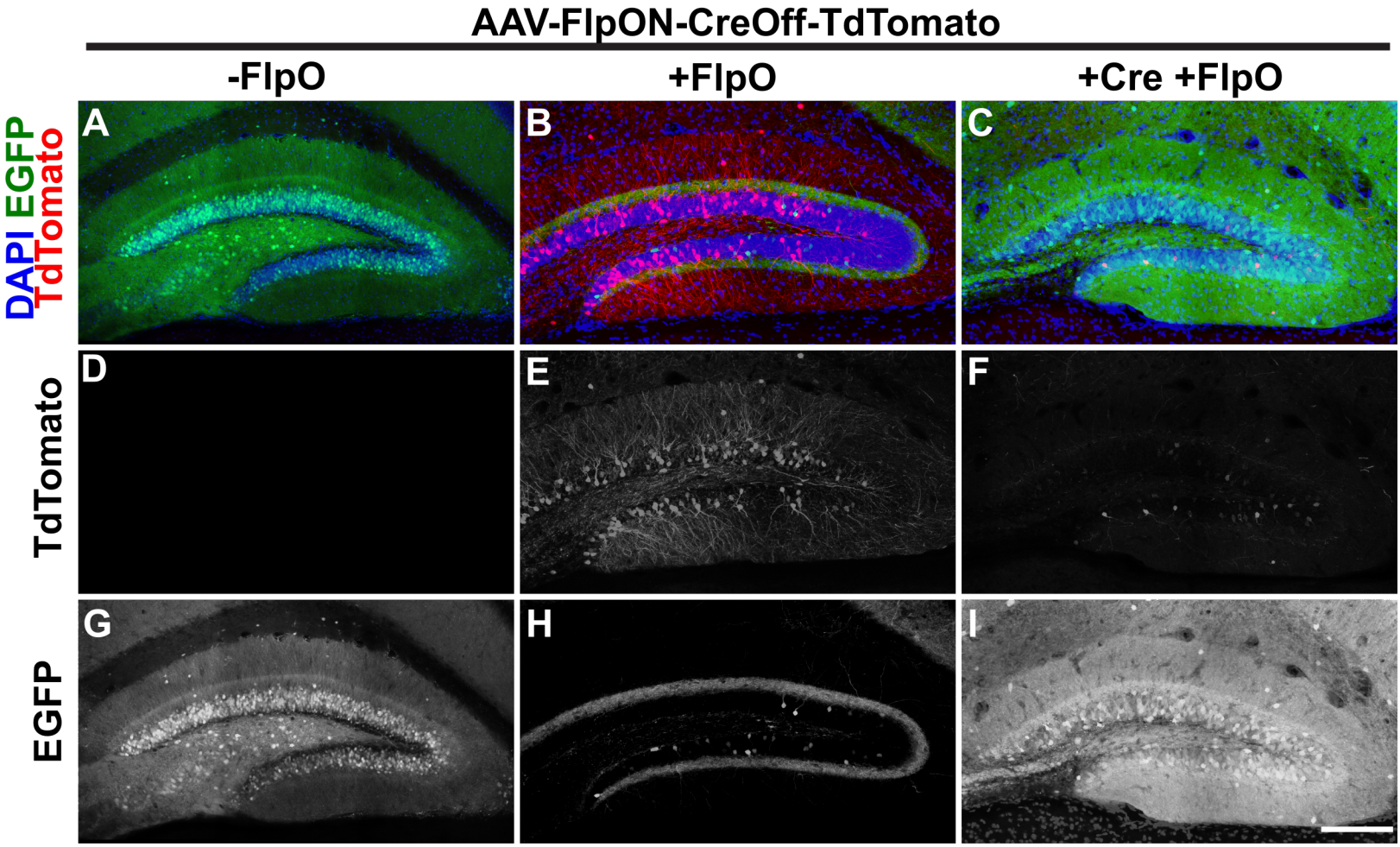
AAV-FlpON-CreOff-TdTomato
-FlpO
+FlpO
+Cre +FlpO
DAPI EGFP
TdTomato
A
B
C
TdTomato
D
E
F
EGFP
G
H
I

Fig5

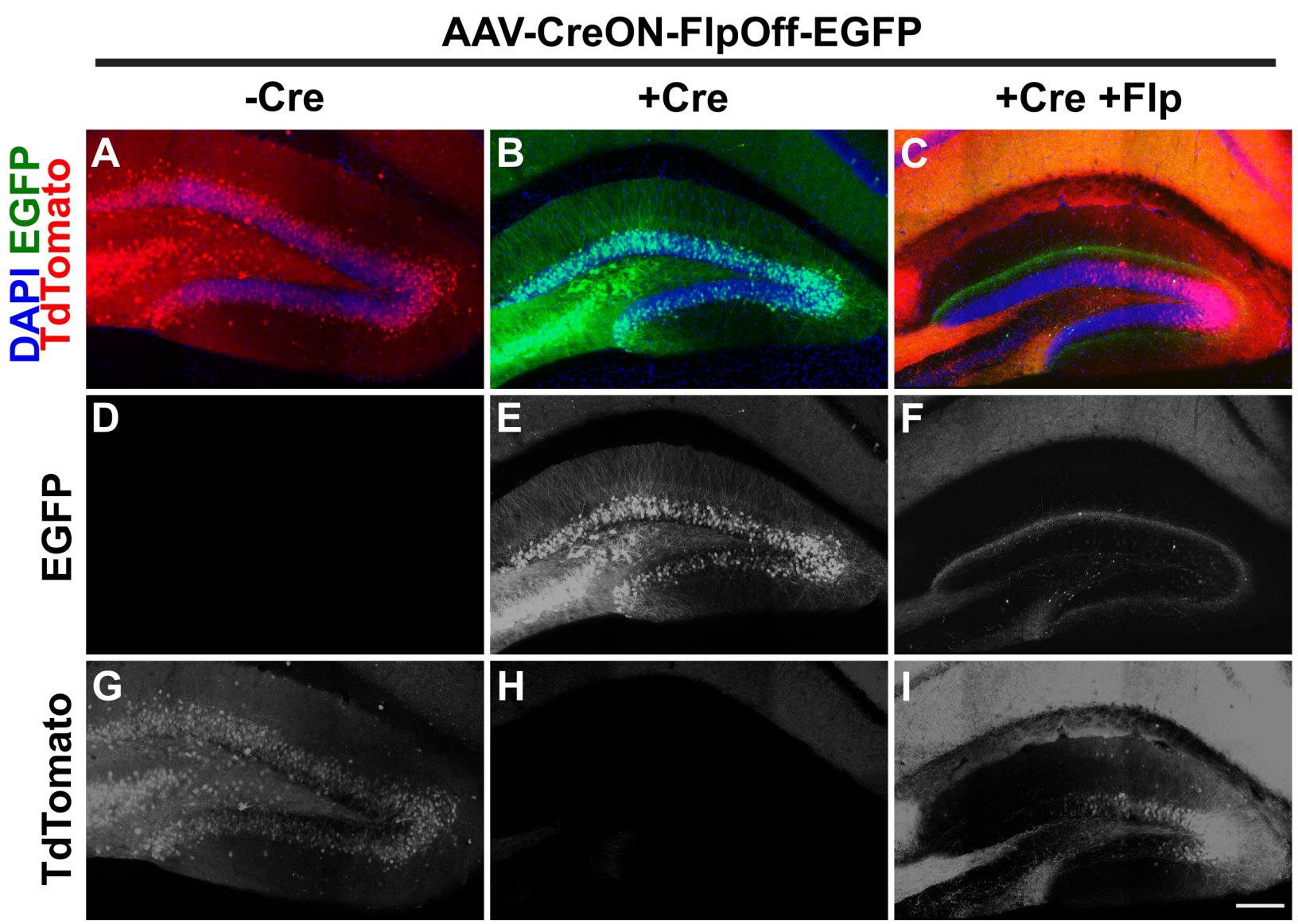
AAV-CreON-FlpOff-EGFP
-Cre
+Cre
+Cre +Flp
DAPI EGFP
TdTomato
EGFP
TdTomato
A
B
C
D
E
F
G
H
I

Fig6

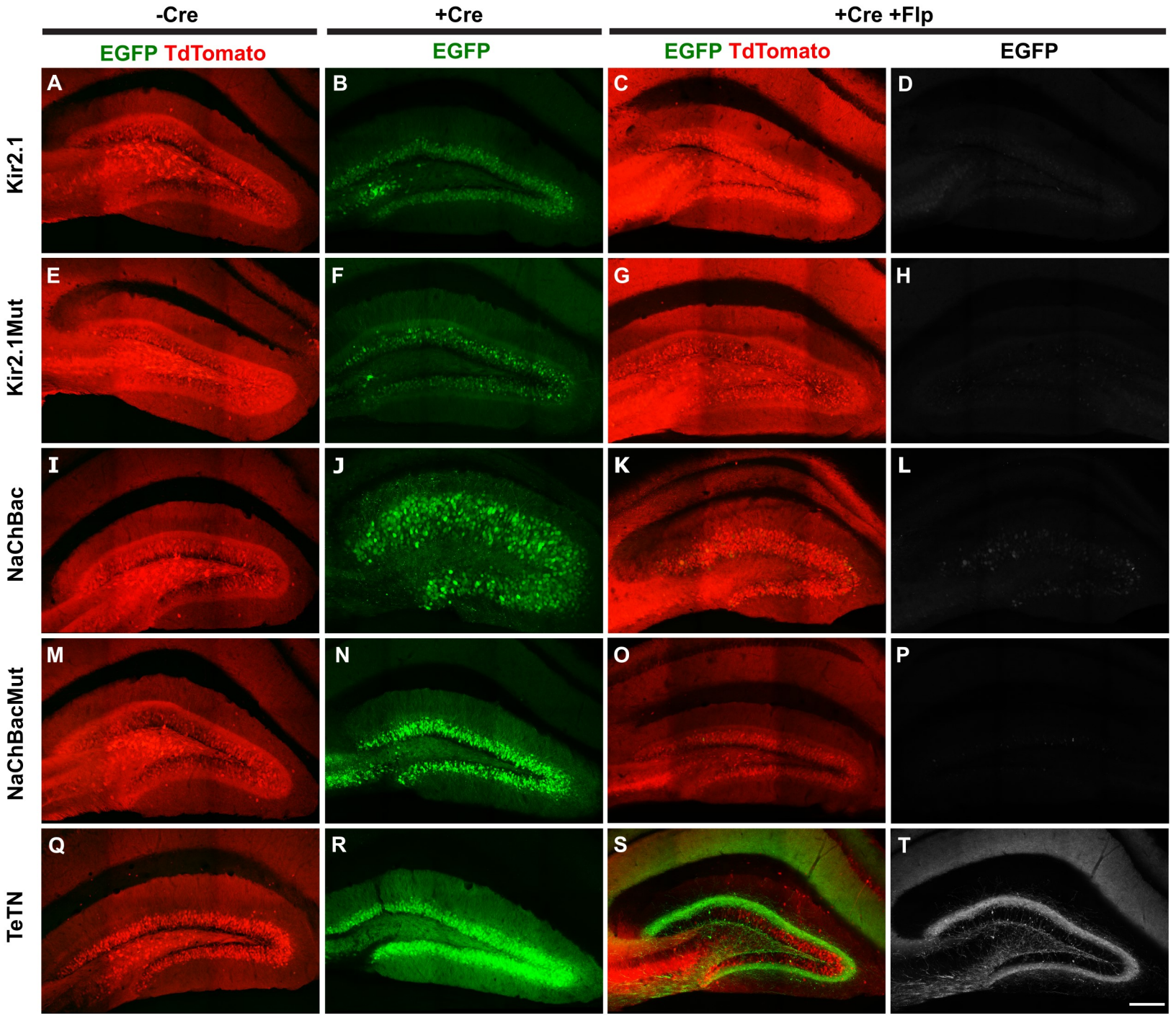
-Cre
+Cre
+Cre +Flp
EGFP TdTomato
EGFP
EGFP TdTomato
EGFP
Kir2.1
Kir2.1Mut
NaChBac
NaChBacMut
TeTN
A
B
C
D
E
F
G
H
I
J
K
L
M
N
O
P
Q
R
S
T

Fig7

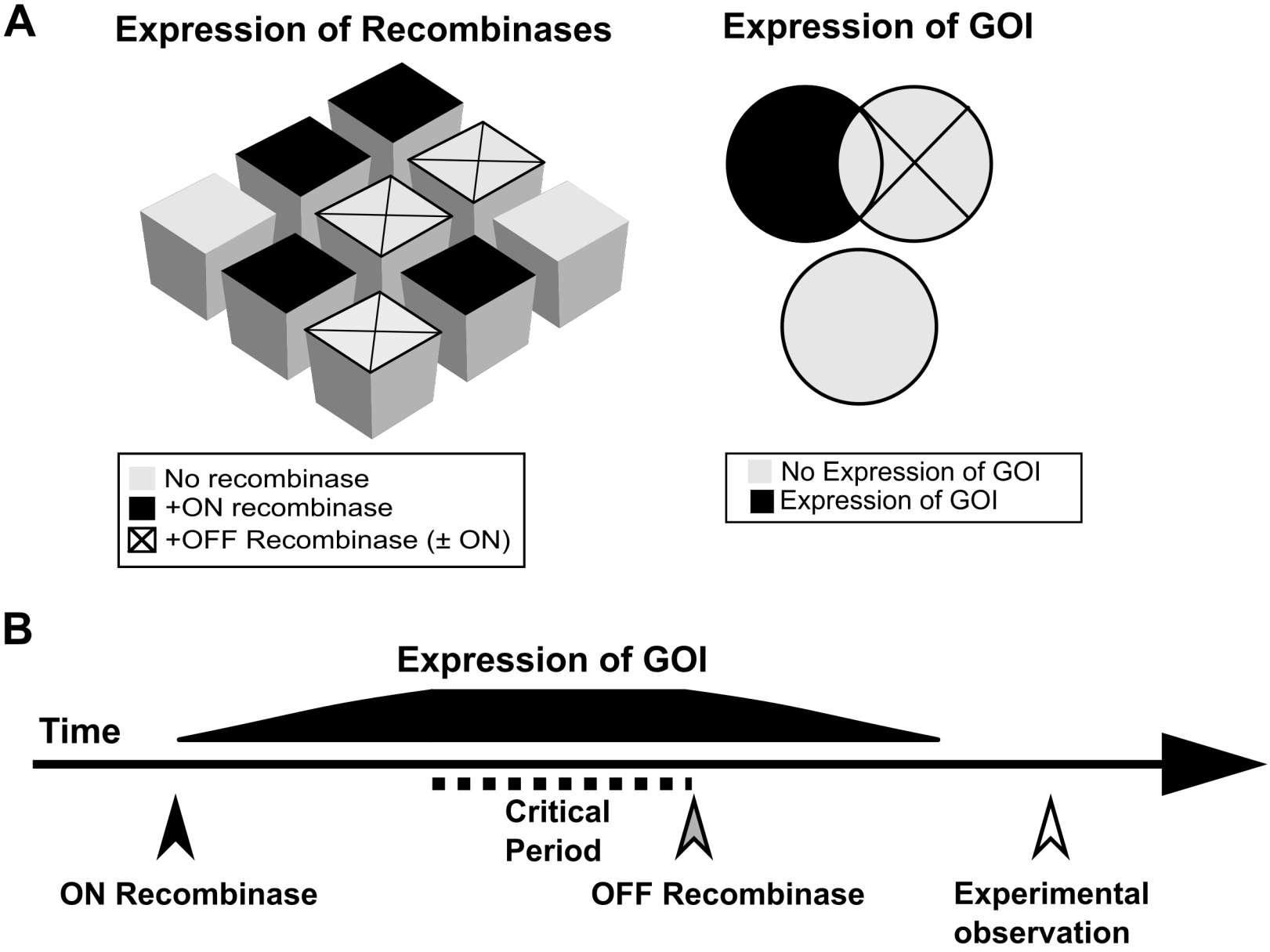
A
Expression of Recombinases
Expression of GOI
No recombinase
+ON recombinase
+OFF Recombinase (± ON)
No Expression of GOI
Expression of GOI
B
Expression of GOI
Time
Critical
Period
ON Recombinase
OFF Recombinase
Experimental
observation

Fig8